

01 Jan 1981

## Excitation Transfer Collisions And Electron Seeding Processes In A Resonantly Excited Sodium Vapor

D. J. Krebs

Laird D. Schearer

*Missouri University of Science and Technology*

Follow this and additional works at: [https://scholarsmine.mst.edu/phys\\_facwork](https://scholarsmine.mst.edu/phys_facwork)

 Part of the [Physics Commons](#)

---

### Recommended Citation

D. J. Krebs and L. D. Schearer, "Excitation Transfer Collisions And Electron Seeding Processes In A Resonantly Excited Sodium Vapor," *The Journal of Chemical Physics*, vol. 75, no. 7, pp. 3340 - 3344, American Institute of Physics, Jan 1981.

The definitive version is available at <https://doi.org/10.1063/1.442487>

This Article - Journal is brought to you for free and open access by Scholars' Mine. It has been accepted for inclusion in Physics Faculty Research & Creative Works by an authorized administrator of Scholars' Mine. This work is protected by U. S. Copyright Law. Unauthorized use including reproduction for redistribution requires the permission of the copyright holder. For more information, please contact [scholarsmine@mst.edu](mailto:scholarsmine@mst.edu).

RESEARCH ARTICLE | OCTOBER 01 1981

## Excitation transfer collisions and electron seeding processes in a resonantly excited sodium vapor

D. J. Krebs; L. D. Schearer



*J. Chem. Phys.* 75, 3340–3344 (1981)

<https://doi.org/10.1063/1.442487>

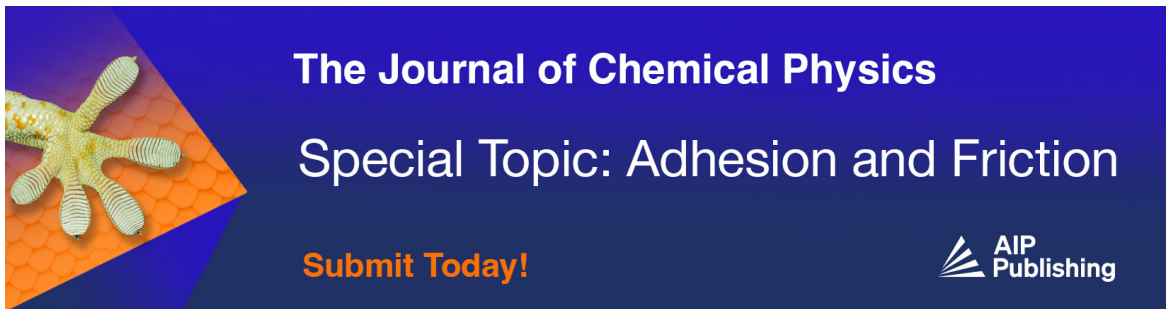


View  
Online





Export  
Citation

CrossMark



**The Journal of Chemical Physics**  
**Special Topic: Adhesion and Friction**  
**Submit Today!**



# Excitation transfer collisions and electron seeding processes in a resonantly excited sodium vapor<sup>a)</sup>

D. J. Krebs and L. D. Schearer

Department of Physics, University of Missouri-Rolla, Rolla, Missouri 65401  
(Received 1 June 1981; accepted 26 June 1981)

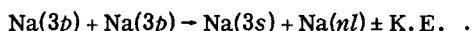
A dense sodium vapor in a high pressure buffer of argon has been simultaneously excited by short (4 ns) laser pulses from two lasers: the first tuned to one of the *D* line transitions at 589 nm and the second tuned to the photoionization threshold of the *3p* states near 406 nm. The temporal evolution of the system was studied with and without the photoionizing laser pulses. At early times ( $\sim 100$  ns) excited state populations are determined by energy transfer collisions between two laser-excited *3p* atoms while the ion/electron density is controlled by superelastic heating of "seed" electrons followed by electron impact ionization of excited state atoms. At late times ( $\sim 1 \mu\text{s}$ ) excited state populations are controlled by collisional-radiative recombination processes. Excitation transfer rates into the *4d*, *5d*, *6d*, and *6s* levels are measured.

## I. INTRODUCTION

A number of interesting effects occur when a dense sodium vapor is excited by laser radiation tuned to one of the *D* lines. In particular, (1) complete ionization has been observed when high power, pulse lasers are employed<sup>1</sup> and (2) surprisingly high densities of atoms are observed in the *nd* ( $n = 3, 4, 5$ ) and *ns* ( $n = 5, 6$ ) levels when a cw laser is employed.<sup>2</sup>

Theoretical calculations<sup>3</sup> indicate that the ionization present in the first case is due to electron heating via superelastic collisions followed by electron impact ionization. A small initial number of electrons (seed electrons) is supplied by several, comparatively weak mechanisms including associative ionization and two photon ionization of the *3p* state atoms.

The mechanisms responsible for the observations in the second case are, perhaps, less well understood. Allegrini *et al.* attributed the excited atom densities to collisions involving two *3p* atoms<sup>2</sup>:



While such an excitation transfer mechanism explains an apparent dependence of the  $\text{Na}(nl)$  density on the square of the *3p* density, there was some doubt whether the cross section for this process is large enough to account for the  $\text{Na}(nl)$  densities observed. Bearman and Levanthal,<sup>4</sup> in an experiment similar to that of Allegrini *et al.* did not observe excitation of levels lying more than  $\sim 3kT$  above the energy of two  $\text{Na}(3p)$  atoms.

The interplay of excitation transfer collisions and electron seeding processes is possible with both cw excitation and excitation with pulsed lasers. In the experiment described here we were able to separate the excitation transfer effects from the effects of the electron impact excitation and ionization by observing the time dependent fluorescence decay from various excited states under two sets of initial conditions: (1) one in which the seed electron density was less than  $10^7 \text{ cm}^{-3}$  and (2) one in which the seed electron density was  $\approx 10^{12} \text{ cm}^{-3}$ . In both cases the initial density of *3p* atoms was about  $10^{15} \text{ cm}^{-3}$ . From differences in the behavior of

the excited state populations under these two conditions we were able to distinguish between processes involving electron collisions and those which do not. In order to observe these effects on a time resolved basis, we used short (4 ns) laser pulses to excite the *3p* states and create the initial electron density. The experimental arrangement is shown in Fig. 1. Kopystynska and Kowalczyk<sup>5</sup> had earlier used short laser pulses to excite the *D* lines and observe subsequent radiative emission from excited *nd* and *ns* states; however, they made no attempt to independently vary the seed electron concentration by using a second ionizing laser pulse as is described in this experiment.

## II. APPARATUS

The reaction cell was a commercial stainless steel cross fitted with sapphire windows on three sides. The sapphire windows were brazed to KOVAR sleeves which were then welded onto CONFLAT flanges. A high conductance bakeable valve connected the cell to a vacuum and gas handling system. The cell was baked for 24 h, at  $400^\circ\text{C}$ , on a system with a base pressure of  $5 \times 10^{-7}$  Torr. A high purity sodium ampoule was crushed in a cold finger and research grade argon was admitted to the desired pressure, typically  $\sim 1$  atm. The argon buffer served two purposes: (1) to broaden the resonance absorption line sufficiently that it matched the laser bandwidth, and (2) to eliminate the diffusion loss of ions, electrons, and excited atoms from the observation region during the course of the experiment. The cell was typically operated at a temperature of  $400^\circ\text{C}$  with a cold finger temperature of  $360^\circ\text{C}$ .

Two  $\text{N}_2$  pumped dye lasers provided 4 ns, 50  $\mu\text{J}$  pulses at their respective wavelengths (589 and 406 nm). The 589 nm laser is tuned to excite one of the  $3^2P$  sodium levels. The 406 nm laser photons have just sufficient energy to photoionize the *3p* atom. The bandwidths were approximately  $0.4 \text{ \AA}$  (FWHM). The beams passed anti-parallel through opposing windows and were focused at the center of the cell by positive lenses ( $f = 35 \text{ cm}$ ) to  $\sim 0.3 \text{ mm}$  spots. The beam divergences were sufficiently small over the observation region that a very nearly cylindrical column of excited vapor was created. A third window permitted monitoring the fluorescence at

<sup>a)</sup> Research supported by the Office of Naval Research.

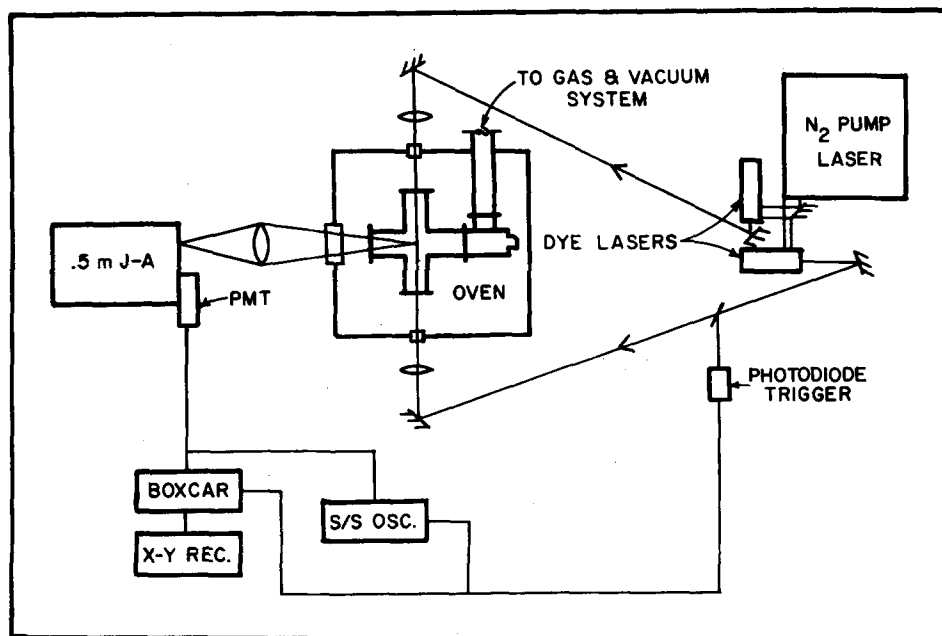


FIG. 1. Schematic of the apparatus.

90° to the axis of the excited region. The fluorescence was monitored by a S-20 photomultiplier (with fast voltage divider chain) coupled to a 0.5 m Jarrell-Ash monochromator. The signal was analyzed by a PAR 160 boxcar integrator or a TEC 5441 storage oscilloscope with a fast sampling head.

### III. EXPERIMENTAL OBSERVATIONS

Figure 2 shows the fluorescence of the  $5d-3p$  transition vs time when both lasers are employed. The optical emission from the cell consists of two components: a strong initial fluorescence pulse of approximately 100 ns duration followed by the rise and slow decay of fluorescence due to excited states created in the three-body, electron stabilized recombination process which extended beyond 20  $\mu\text{s}$ . Figure 3 is a wavelength scan of the recombination fluorescence 2  $\mu\text{s}$  after the lasers

have fired. The detecting apparatus was calibrated against the emission of a standard quartz-iodine lamp to permit absolute measurements of the excited state densities. A Saha-Boltzmann plot of the absolute excited state densities for levels above the  $7d$  state yields an electron density of  $1 \times 10^{14} \text{ cm}^{-3}$  at 2  $\mu\text{s}$  after the lasers are fired.<sup>6</sup> Stark shifts of the  $6^2D-3^2P$  and  $7^2D-3^2P$  due to the electrons were also measured. It was necessary in a separate experiment to determine the shift due to the argon buffer gas<sup>7</sup> and subtract the two shifts to obtain the shift due to electron collisions. The results agreed well with Griem's predictions for

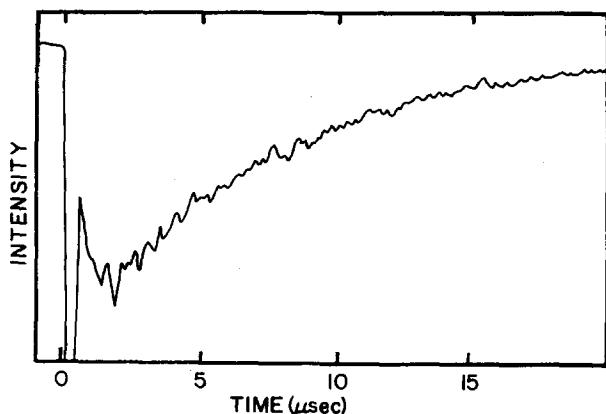


FIG. 2. Fluorescence intensity vs time after laser excitation for the  $5d-3p$  transition with both lasers employed. The early fluorescence peak, which is off-scale, is approximately 20 times more intense than the peak of the recombination fluorescence at  $t = 2 \mu\text{s}$ .

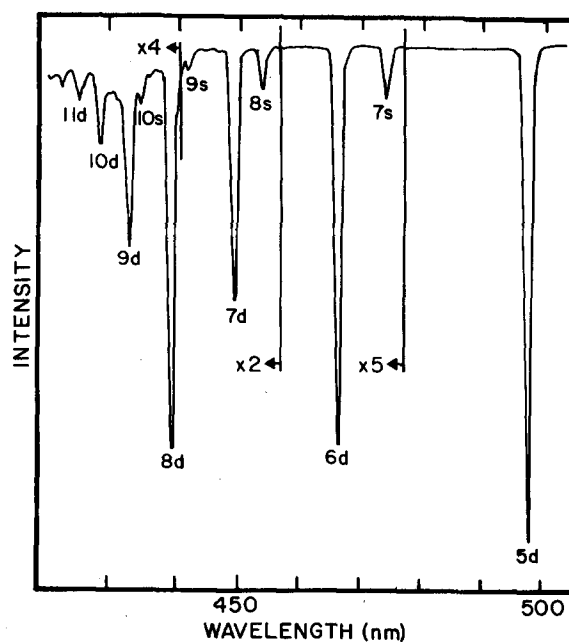


FIG. 3. Recombination fluorescence at  $t = 2 \mu\text{s}$  vs wavelength. Scan resolution is 0.8 nm (FWHM).

$N_e \approx 10^{14} \text{ cm}^{-3}$ .<sup>8</sup> For reasons detailed below, the electron density immediately after the lasers have fired is considerably smaller than it is  $2 \mu\text{s}$  later.

With the ionizing (406 nm) laser off, the recombination fluorescence disappeared, indicating an absence of strong ionization. The early fluorescence pulse generally remained albeit altered in magnitude and shape. Less than one percent of the ionizing laser pulse at 406 nm is absorbed.

Figure 4 shows the level of the  $3p-3s$  resonance fluorescence with and without the ionizing laser pulse. It may be seen in Fig. 4, and is apparent in traces from the fast oscilloscope, that the  $3p$  population is not significantly changed by the ionizing laser in the first 30 ns after the lasers have fired. At later times, however, the  $3p$  population is depleted about 16% by the presence of the ionizing laser pulses, which are virtually synchronous with the resonant laser pulses. Thus, we believe that the ionization is enhanced by the electron seeding process suggested by Measures, with direct photoionization by the ionizing laser providing the seed electrons. In this model, the energy of any free (seed) electrons is rapidly increased by superelastic collisions with the large density of excited  $3p$  atoms. Subsequently, ionization proceeds via electron impact excitation and ionization of the excited atoms. The number of seed electrons provided by the ionizing laser is  $\sim 10^{12} \text{ cm}^{-3}$  since the photoionization cross section is large near threshold.

The 589 and 406 nm lasers can excite high vibrational levels of the  $A^1\Sigma$  and  $B^1\Pi$  states of the dimer, respectively. Some weak dimer emission was seen in the early fluorescence. The recombination fluorescence and early atomic fluorescence disappeared when the resonant laser was detuned by a few angstroms, indicating a dependence of these signals on the presence of large concentrations of  $\text{Na}(3p)$  atoms. Thus dimer absorption does not play a role in the excitation and ionization processes in this experiment.

Figure 4 shows the strong initial fluorescence pulse for several transitions both with and without the ionizing laser. Without the ionizing laser, the rise of the fluorescence pulse is rapid for the  $4d-3p$  fluorescence and considerably slower for the  $5d-3p$  and  $6d-3p$  transitions. With the ionizing laser on, the  $4d$  population declines by about 25%. The  $5d$  and  $6d$  populations exhibit a more rapid rise and decay, than they do with the ionizing laser off. We measured the population densities corresponding to each level based on the calibration of our detection system as previously mentioned.

With the ionizing laser on, the electron density is several orders of magnitude greater than when it is off. The electron temperature is not altered greatly, however, because the electron temperature is controlled by the  $3p$  population<sup>3</sup> which is not greatly changed. If the production of atoms in the  $ns$  and  $nd$  states were due to electron impact excitation, the fluorescence from these levels would increase dramatically when the ionizing laser is on. This does not occur and therefore electron collisions are not the source of the  $nd$  and  $ns$  populations in this experiment.

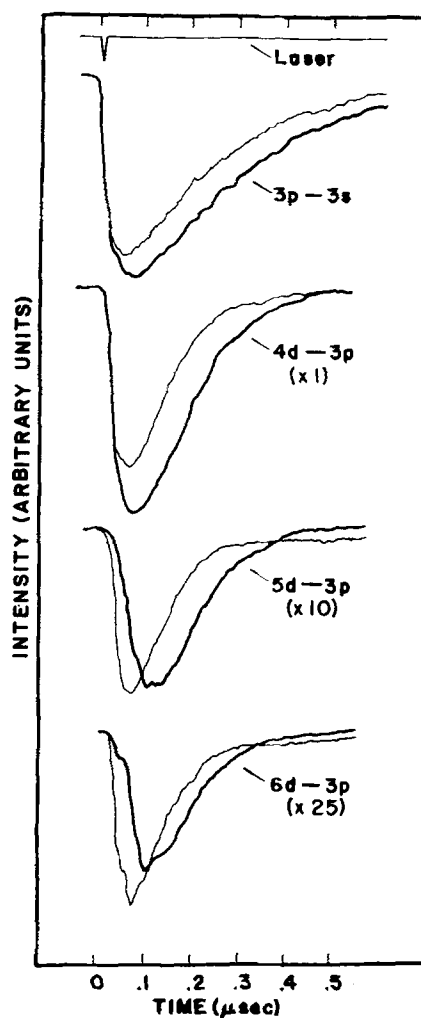


FIG. 4. Early fluorescence intensity for various transitions vs time. Resonance fluorescence for the  $3p-3s$  transition is not calibrated relative to that of the  $nd-3p$  transitions. Otherwise the relative intensities are as indicated. Lighter traces were taken with both lasers employed. Dark traces were taken with only the laser tuned to 589 nm employed.

Traces from the fast oscilloscope indicate that the rise of the  $4d$  population occurs about 10 ns after the laser pulse has passed and does not peak until about 30 ns after the  $3p$  population has peaked. Since the laser pulses are only 4 ns in duration (FWHM), any radiative absorption process involving the laser pulses cannot be responsible for the  $4d$  population. We considered and excluded the possibility that trapped resonance radiation might be absorbed in the far wings of the  $3p-4d$  and  $3p-5s$  transitions. Since the photon energy density of the trapped radiation is several orders of magnitude smaller than that of the laser, this explanation does not fit the observed time dependence.

#### IV. DISCUSSION AND CONCLUSION

The excitation transfer process originally proposed by Allegrini *et al.*<sup>2</sup>



appears to be the primary source of the  $4d$ ,  $5d$ ,  $6d$ , and

6s population in the early afterglow. We thus write

$$N_{3p}(t) = N_{3p}(0) \exp(-t/\tau_{3p}^*), \quad (2)$$

where  $\tau_{3p}^*$  is the trapped lifetime of the  $3p$  state, and

$$\frac{dN_{nl}(t)}{dt} = -\frac{N_{nl}}{\tau_{nl}} + k_{nl} [N_{3p}(t)]^2, \quad (3)$$

where  $\tau_{nl}$  is the effective lifetime of the  $nl$  state and  $k_{nl}$  is the rate constant for the production of the  $N_{nl}$  atoms by the excitation transfer process of Eq. (1). Equation (3) is easily solved to yield

$$N_{nl}(t) = k_{nl} [N_{3p}(0)]^2 \tau_{3p}^* \tau_{nl} (\tau_{3p}^* - 2\tau_{nl})^{-1} \times [\exp(-2t/\tau_{3p}^*) - \exp(-t/\tau_{nl})]. \quad (4)$$

Kopystynska<sup>5</sup> and Kowalczyk showed that Eq. (4) fits the time dependence of their experimental data quite well. We also found that Eq. (4) fits our data as shown in Fig. 5 although the effective decay rates are shorter than the natural radiative lifetimes. This is not surprising considering the biexponential form of the decay from these excited levels at our high buffer pressures.<sup>9</sup>

If this interpretation is correct, we can obtain estimates of  $K_{nl}$  by fitting Eq. (4) to the experimental curves. A fit to the  $4d-3p$  observations is shown in Fig. 5. From this we obtain  $K_{4d} = 1 \times 10^{-12} \text{ cm}^3 \text{ s}^{-1}$  and  $\tau_{4d} = 39 \text{ ns}$ . Extending this analysis to the other states, we obtain the data in Table I. The absolute uncertainty of the  $K_{nl}$  measurements is about an order of magnitude, due principally to uncertainty in the  $3p$  population. The relative accuracy of these data should be quite good since there is little uncertainty in the relative populations in the  $nd$  and  $ns$  states.

Kowalczyk<sup>11</sup> has modeled the excitation transfer collision of two Na( $3p$ ) atoms using adiabatic molecular potentials. In this model, the cross section for excitation transfer depends strongly on the electric dipole matrix elements connecting the Na( $3p$ ) level to the highly excited Na( $nl$ ) level. Since for excitation to a Na( $np$ ) level,

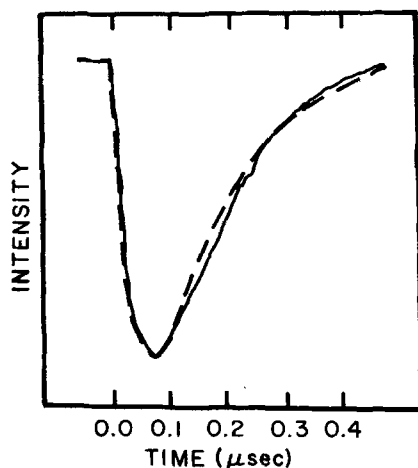


FIG. 5. Fluorescence intensity of the  $4d-3p$  transition vs time. The solid curve is experimentally derived. The dashed curve was calculated using Eq. (4).

TABLE I. Values of  $k_{nl}$  and magnitudes of the energy defects.

Level	$k_{nl} (\text{cm}^3 \text{ s}^{-1})$	$(E_{nl} - 2E_{3p})/kT$
$4d^a$	$1 \times 10^{-12}$	1.2
$4d^b$	$5 \times 10^{-11}$	1.2
$5d^a$	$5.2 \times 10^{-14}$	6.1
$6d^a$	$8.6 \times 10^{-15}$	8.7
$6s^a$	$7.6 \times 10^{-15}$	4.8
$4p^c$	$6.1 \times 10^{-16}$	-10.8
$5p^d$	$7 \times 10^{-18}$	3.1

<sup>a</sup>This work,  $T = 397^\circ \text{C}$ .

<sup>b</sup>Calculated from Ref. 11,  $T = 377^\circ \text{C}$ .

<sup>c</sup>Taken from Ref. 10,  $T = 214^\circ \text{C}$ .

<sup>d</sup>Taken from Ref. 10,  $T = 243^\circ \text{C}$ .

this matrix element is zero, corresponding to a dipole-forbidden transition, we expect that the rate constants for  $4p$  and  $5p$  formation measured by Kushawaha and Levanthal<sup>10</sup> to be significantly smaller than the  $4d$ ,  $5d$ ,  $6d$ , and  $6s$  rate constants reported here. The calculated cross section for excitation transfer to the  $4d$  state is  $6.1 \times 10^{-18} \text{ cm}^2$  at  $T = 650^\circ \text{K}$ .<sup>11</sup> This corresponds to a rate constant of  $5 \times 10^{-11} \text{ cm}^3 \text{ s}^{-1}$  which is to be compared with the value of  $1 \times 10^{-12} \text{ cm}^3 \text{ s}^{-1}$  obtained in this experiment. The results are summarized in Table I.

We note that the rate constants reported in Table I decrease dramatically as the energy defect increases from 1.2 to 8.7  $kT$ . The reduction in the rate constant follows approximately the reduction in the fraction of atoms in a Boltzmann distribution which have kinetic energies greater than the energy defect. This behavior is consistent with the theoretical model of Kowalczyk.

We note that the  $nd$  levels are strongly coupled to higher angular momentum levels by mixing collisions with the buffer gas.<sup>9</sup> As a result, the degeneracy of these levels is effectively  $2N^2 - 8$ . The net population in all these excited levels represents a significant pool of target atoms for electron impact ionization. Perhaps the electron seeding models should incorporate excitation transfer mechanisms as more rate constant data becomes available.

In summary, we find that the populations of the  $4d$ ,  $5d$ ,  $6d$ , and  $6s$  states in the early afterglow are due to energy transfer collisions between two  $3p$  atoms. The ionization of the Na results from superelastic heating of the seed electrons (produced by photoionization) in collision with the  $3p$  atoms and subsequent ionization by electron impact.

<sup>1</sup>(a) T. B. Lucatorto and T. J. McIlrath, Phys. Rev. Lett. 37, 428 (1976); (b) T. J. McIlrath and T. B. Lucatorto, *ibid.* 38, 1390 (1977).

<sup>2</sup>M. Allegrini, G. Alzetta, A. Kopystynska, L. Moi, and G. Orriols, Opt. Commun. 19, 96 (1976).

<sup>3</sup>R. M. Measures and P. T. Cardinal, Phys. Rev. A 23, 804 (1981).

<sup>4</sup>G. H. Bearman and J. J. Levanthal, Phys. Rev. Lett. 41,

1227 (1978).

- <sup>5</sup>A. Kopystynska and P. Kowalczyk, *Opt. Commun.* **25**, 351 (1978).
- <sup>6</sup>L. K. Lam and L. D. Schearer, *Chem. Phys. Lett.* **60**, 130 (1978).
- <sup>7</sup>D. Krebs and L. D. Schearer, 33rd Annual Gaseous Electronics Conference, University of Oklahoma, October, 1980 (unpublished).

- <sup>8</sup>H. R. Griem, *Plasma Spectroscopy* (McGraw-Hill, New York, 1964).
- <sup>9</sup>T. F. Gallagher, S. A. Edelstein, and R. M. Hill, *Phys. Rev. A* **15**, 1945 (1977).
- <sup>10</sup>V. S. Kushawaha and J. J. Leventhal, *Phys. Rev. A* **22**, 2468 (1980).
- <sup>11</sup>P. Kowalczyk, *Chem. Phys. Lett.* **68**, 203 (1975).